

TITLE

Ilia Kohanovski^a, Uri Obolski^{b,c}, and Yoav Ram^{a,*}

^aSchool of Computer Science, Interdisciplinary Center Herzliya, Herzliya 4610101, Israel

^bSchool of Public Health, Tel Aviv University, Tel Aviv 6997801, Israel

^cPorter School of the Environment and Earth Sciences, Tel Aviv University, Tel Aviv 6997801, Israel

*Corresponding author: yoav@yoavram.com

May 4, 2020

Abstract

Lorem ipsum dolor sit amet, consectetur adipiscing elit. Ut purus elit, vestibulum ut, placerat ac, adipiscing vitae, felis. Curabitur dictum gravida mauris. Nam arcu libero, nonummy eget, consectetur id, vulputate a, magna. Donec vehicula augue eu neque. Pellentesque habitant morbi tristique senectus et netus et malesuada fames ac turpis egestas. Mauris ut leo. Cras viverra metus rhoncus sem. Nulla et lectus vestibulum urna fringilla ultrices. Phasellus eu tellus sit amet tortor gravida placerat. Integer sapien est, iaculis in, pretium quis, viverra ac, nunc. Praesent eget sem vel leo ultrices bibendum. Aenean faucibus. Morbi dolor nulla, malesuada eu, pulvinar at, mollis ac, nulla. Curabitur auctor semper nulla. Donec varius orci eget risus. Duis nibh mi, congue eu, accumsan eleifend, sagittis quis, diam. Duis eget orci sit amet orci dignissim rutrum.

18 Introduction

19 The COVID-19 pandemic has resulted in implementation of extreme non-pharmaceutical interventions
20 (NPIs) in many affected countries. These interventions, from social distancing to lockdowns, are
21 applied in a rapid and widespread fashion. The NPIs are designed and assessed using epidemiological
22 models, which follow the dynamics of the viral infection to forecast the effect of different mitigation and
23 suppression strategies on the levels of infection, hospitalization, and fatality. These epidemiological
24 models usually assume that the effect of NPIs on disease transmission begins at the officially declared
25 date (e.g. Flaxman et al.⁵, Gatto et al.⁷, Li et al.⁹).

26 Adoption of public health recommendations is often critical for effective response to infectious dis-
27 eases, and has been studied in the context of HIV⁸ and vaccination^{3,12}, for example. However,
28 behavioral and social change does not occur immediately, but rather requires time to diffuse in the
29 population through media, social networks, and social interactions. Moreover, compliance to NPIs
30 may differ between different interventions and between people. For example, in a survey of 2,108
31 adults in the UK during Mar 2020, Atchison et al.² found that those over 70 years old were more likely
32 to adopt social distancing than young adults (18-34 years old), and that those with lower income were
33 less likely to be able to work from home and to self-isolate. Furthermore, compliance to NPIs may be
34 impacted by risk perception, as perceived by the number of domestic cases or even by reported cases in
35 other regions and countries. Interestingly, the perceived risk of COVID-19 infection has likely caused
36 a reduction in the number of influenza-like illness cases in the US starting from mid-February¹³.

37 Here, we hypothesize that there is a significant difference between the official start of NPIs and their
38 adoption by the public and therefore their effect on transmission dynamics. We use a *Susceptible-*
39 *Exposed-Infected-Recovered* (SEIR) epidemiological model and *Markov Chain Monte Carlo* (MCMC)
40 parameter estimation framework to estimate the effective start date of NPIs from publicly available
41 COVID-19 case data in several geographical regions. We compare these estimates to the official
42 dates and find both delayed and advanced effect of NPIs on COVID-19 transmission dynamics. We
43 conclude by demonstrating how differences between the official and effective start of NPIs can confuse
44 assessments of the effectiveness of the NPIs in a simple epidemic control framework.

45 Models and Methods

46 **Data.** We use daily confirmed case data $\mathbf{X} = (X_1, \dots, X_T)$ from several different countries. These
47 incidence data summarize the number of individuals X_t tested positive for SARS-CoV-2 RNA (using
48 RT-qPCR) at each day t . Data was retrieved for X regions, see Table 1 for details and references.
49 In regions in which there were multiple sequences of days with zero confirmed cases (e.g. France),
50 we cropped the data to begin with the last sequence so that our analysis focuses on the first sustained
51 outbreak rather than isolated imported cases.

Region	Start date	End date	Reference
Austria	X Feb		Flaxman et al. ⁵
Wuhan, China	10 Jan	8 Feb	Pei and Shaman ¹⁰

Table 1: Reference for confirmed cases incidence data. All dates in 2020.

52 **SEIR model.** We model SARS-CoV-2 infection dynamics by following the number of susceptible
53 S , exposed E , reported infected I_r , and unreported infected I_u individuals in a population of size N .
54 This model distinguishes between reported and unreported infected individuals: the reported infected

55 are those that have enough symptoms to eventually be tested and thus appear in daily case reports, to
 56 which we fit the model.

57 Susceptible (S) individuals become exposed due to contact with reported or unreported infected
 58 individuals (I_r or I_u) at a rate β_t or $\mu\beta_t$. The parameter $0 < \mu < 1$ represents the decreased transmission
 59 rate from unreported infected individuals, who are often subclinical or even asymptomatic. The
 60 transmission rate $\beta_t \geq 0$ may change over time t due to behavioural changes of both susceptible
 61 and infected individuals. Exposed individuals, after an average incubation period of Z days, become
 62 reported infected with probability α_t or unreported infected with probability $(1 - \alpha_t)$. The reporting
 63 rate $0 < \alpha_t < 1$ may also change over time due to changes in human behavior. Infected individuals
 64 remain infectious for an average period of D days, after which they either recover, or becomes ill
 65 enough to be quarantined. They therefore no longer infect other individuals, and the model does not
 66 track their frequency. The model is described by the following equations:

$$\begin{aligned}
 \frac{dS}{dt} &= -\beta_t S \frac{I_p}{N} - \mu\beta_t S \frac{I_u}{N} \\
 \frac{dE}{dt} &= \beta_t S \frac{I_p}{N} + \mu\beta_t S \frac{I_u}{N} - \frac{E}{Z} \\
 \frac{dI_r}{dt} &= \alpha_t \frac{E}{Z} - \frac{I_r}{D} \\
 \frac{dI_u}{dt} &= (1 - \alpha_t) \frac{E}{Z} - \frac{I_u}{D}.
 \end{aligned} \tag{1}$$

68 The initial numbers of exposed $E(0)$ and unreported infected $I_u(0)$ are considered model parameters,
 69 whereas the initial number of reported infected is assumed to be zero $I_r(0) = 0$, and the number of
 70 susceptible is $S(0) = N - E(0) - I_u(0)$. The vector θ of model parameters is

$$\theta = \left(Z, D, \mu, \{\beta_t\}, \{\alpha_t\}, \{p_t\}, E(0), I_u(0) \right). \tag{2}$$

72 This model is inspired by Li et al.⁹ and Pei and Shaman¹⁰, who used a similar model with multiple
 73 regions and constant transmission β and reporting rate α to infer COVID-19 dynamics in China and
 74 the continental US, respectively.

75 **Likelihood function.** The *expected* cumulative number of reported infected individuals until day t
 76 is

$$Y_t = \int_0^t \alpha_s \frac{E(s)}{Z} ds, \quad Y_0 = 0. \tag{3}$$

We assume that reported infected individuals are confirmed and therefore observed in the daily case
 report of day t with probability p_t (note that an individual can only be observed once, and that p_t may
 change over time, but t is a specific date rather than the time elapsed since the individual was infected).
 Hence, we assume that the number of confirmed cases in day t is binomially distributed,

$$X_t \sim \text{Bin}(n_t, p_t),$$

where n_t is the *realized* (rather than expected) number of reported infected individuals yet to appear
 in daily reports by day t . The cumulative number of confirmed cases until day t is

$$\tilde{X}_t = \sum_{i=1}^t X_i, \quad X_0 = 0.$$

Given \tilde{X}_{t-1} , we assume n_t is Poisson distributed,

$$(n_t \mid \tilde{X}_{t-1}) \sim \text{Poi}(Y_t - \tilde{X}_{t-1}), \quad n_1 \sim \text{Poi}(Y_1).$$

78 Therefore, $(X_t | \tilde{X}_{t-1})$ is a binomial conditioned on a Poisson, which reduces to a Poisson with

$$79 \quad (X_t | \tilde{X}_{t-1}) \sim \text{Poi}\left((Y_t - \tilde{X}_{t-1}) \cdot p_t\right), \quad X_1 \sim \text{Poi}(Y_1 \cdot p_1). \quad (4)$$

80 For given vector θ of model parameters (Eq. (2)), we compute the expected cumulative number
 81 of reported infected individuals $\{Y_t\}_{t=1}^T$ for each day (Eq. (3)). Then, since \tilde{X}_{t-1} is a function of
 82 X_1, \dots, X_{t-1} , we can use Eq. (4) to write the probability to observe the confirmed case data $\mathbf{X} =$
 83 (X_1, \dots, X_T) as

$$84 \quad \mathbb{L}(\theta | \mathbf{X}) = P(\mathbf{X} | \theta) = P(X_1 | \theta)P(X_2 | \tilde{X}_1, \theta) \cdots P(X_T | \tilde{X}_{T-1}, \theta). \quad (5)$$

85 This defines a *likelihood function* $\mathbb{L}(\theta | \mathbf{X})$ for the parameter vector θ given the data \mathbf{X} .

86 **NPI model.** To model non-pharmaceutical interventions (NPIs), we set the beginning of the NPIs
 87 to day τ and define

$$88 \quad \beta_t = \begin{cases} \beta, & t < \tau \\ \beta\lambda, & t \geq \tau \end{cases}, \quad \alpha_t = \begin{cases} \alpha_1, & t < \tau \\ \alpha_2, & t \geq \tau \end{cases}, \quad p_t = \begin{cases} 1/9, & t < \tau \\ 1/6, & t \geq \tau \end{cases}, \quad (6)$$

89 where $0 < \lambda < 1$. The values for p_t follow Li et al.⁹, who estimated the average time between infection
 90 and reporting in Wuhan, China, at 9 days before the start of NPIs (Jan 23, 2020) and 6 days after start
 91 of NPIs. The parameter τ is then added to the parameter vector θ (Eq. (2)).

92 **Parameter estimation.** To estimate the parameters θ of our model (Eq. (1)) from the data \mathbf{X} , we
 93 apply a Bayesian inference approach. We define the following flat priors on the model parameters
 94 $P(\theta)$:

$$\begin{aligned} & Z \sim \text{Uniform}(2, 5) \\ & D \sim \text{Uniform}(2, 5) \\ & \mu \sim \text{Uniform}(0.2, 1) \\ & \beta \sim \text{Uniform}(0.8, 1.5) \\ 95 \quad & \lambda \sim \text{Uniform}(0, 1) \\ & \alpha_1, \alpha_2 \sim \text{Uniform}(0.02, 1) \\ & E(0) \sim \text{Uniform}(0, 3000) \\ & I_u(0) \sim \text{Uniform}(0, 3000) \\ & \tau \sim \text{Uniform}(1, T - 1), \end{aligned} \quad (7)$$

96 where T is the number of days in the data \mathbf{X} . Most priors follow Li et al.⁹, except λ , which is used to
 97 enforce that the transmission rates are lower after the start of the NPIs ($\lambda < 1$). The likelihood function
 98 is defined in Eq. (5). The posterior distribution on the model parameters $P(\theta | \mathbf{X})$ is then estimated
 99 using an *affine-invariant ensemble sampler for Markov chain Monte Carlo* (MCMC) implemented in
 100 the *emcee* Python package⁶.

101 **Model selection.** We perform model selection using DIC (deviance information criterion)¹¹,

$$\begin{aligned} 102 \quad & \text{DIC}(\theta, \mathbf{X}) = 2\mathbb{E}[D(\theta)] - D(\mathbb{E}[\theta]) \\ & = 2\log \mathcal{L}(\mathbb{E}[\theta] | \mathbf{X}) - 4\mathbb{E}[\log \mathcal{L}(\theta | \mathbf{X})], \end{aligned} \quad (8)$$

103 where $D(\theta)$ is the Bayesian deviance, and expectations $\mathbb{E}[\cdot]$ are taken over the posterior distribution
 104 $P(\theta | \mathbf{X})$. We compare models by reporting their relative DIC; lower is better.

105 **Source code.** We use Python 3 (Anaconda) with the NumPy, Matplotlib, SciPy, Pandas, Seaborn,
 106 and emcee packages. All source code will be publicly available under a permissive open-source
 107 license at github.com/yoavram-lab/EffectiveNPI.

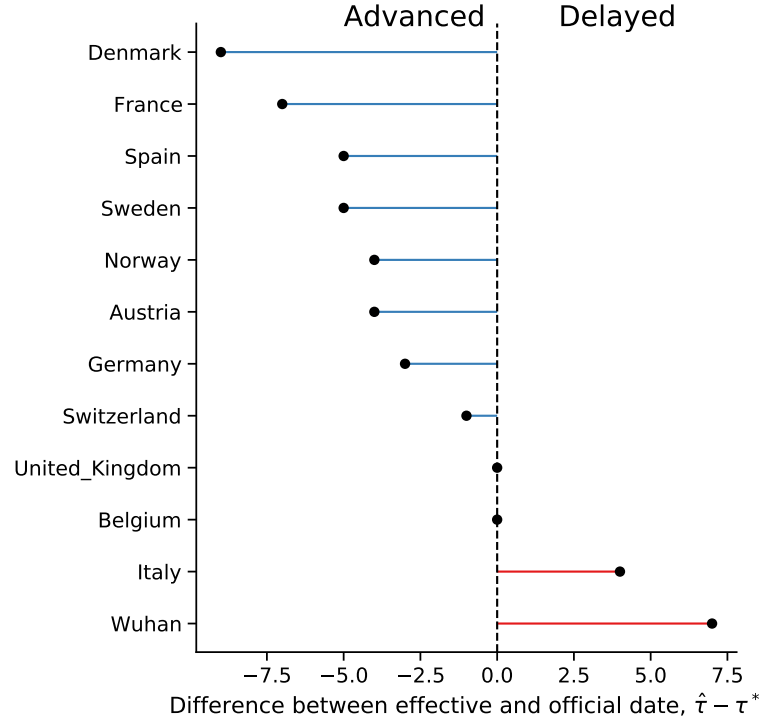


Figure 1: Official and effective start of non-pharmaceutical interventions.

108 Results

109 Several studies have described the effects of non-pharmaceutical interventions in different geographical
 110 regions^{5,7,9}. These studies have assumed that the parameters of the epidemiological model change at
 111 a specific date, as in Eq. (6), and set the change date τ to the official NPI date τ^* . They then fit the
 112 model once for time $t < \tau^*$ and once for time $t \geq \tau^*$ (see [TABLE2](#) for a summary of official NPI
 113 dates.) For example, Li et al.⁹ estimate the dynamics in China before and after τ^* at Jan 23. Thereby,
 114 they effectively estimate (β, α_1) and (λ, α_2) separately. Here we estimate the posterior distribution
 115 $P(\tau | \mathbf{X})$ of the *effective* start date of the NPIs by jointly estimating $\tau, \beta, \lambda, \alpha_1, \alpha_2$ on the entire data
 116 per region (e.g. Italy, Austria), rather than splitting the data at τ^* . We then compute the maximum a
 117 posteriori estimate $\hat{\tau} = \arg\max_{\tau} P(\tau | \mathbf{X})$.

118 We find that a model that considers an NPI (Eq. (6)) is a better fit to the data than a model without an
 119 NPI, i.e. with constant β and α ([\$\Delta DIC > ?\$ for all regions](#).) We compare the official τ^* and effective
 120 $\hat{\tau}$ start of NPIs and find that in most regions the effective start of NPI significantly differs from the
 121 official date (Figure 1): the [75%](#) confidence interval on $\hat{\tau}$ does not include τ^* , and the DIC of the
 122 model with free τ parameter is lower than that of a model with a fixed $\tau \equiv \tau^*$ ([\$\Delta DIC > ?\$](#) .) The
 123 exception that proves the rule is [Switzerland](#).

124 In the following, we describe our findings on delayed and advanced start of NPI in detail.

125 **Delayed effective start of NPI.** In both Wuhan, China, and in Italy we find that our estimated
 126 effective start of NPI $\hat{\tau}$ is significantly later than the official date τ^* (Figure 1).

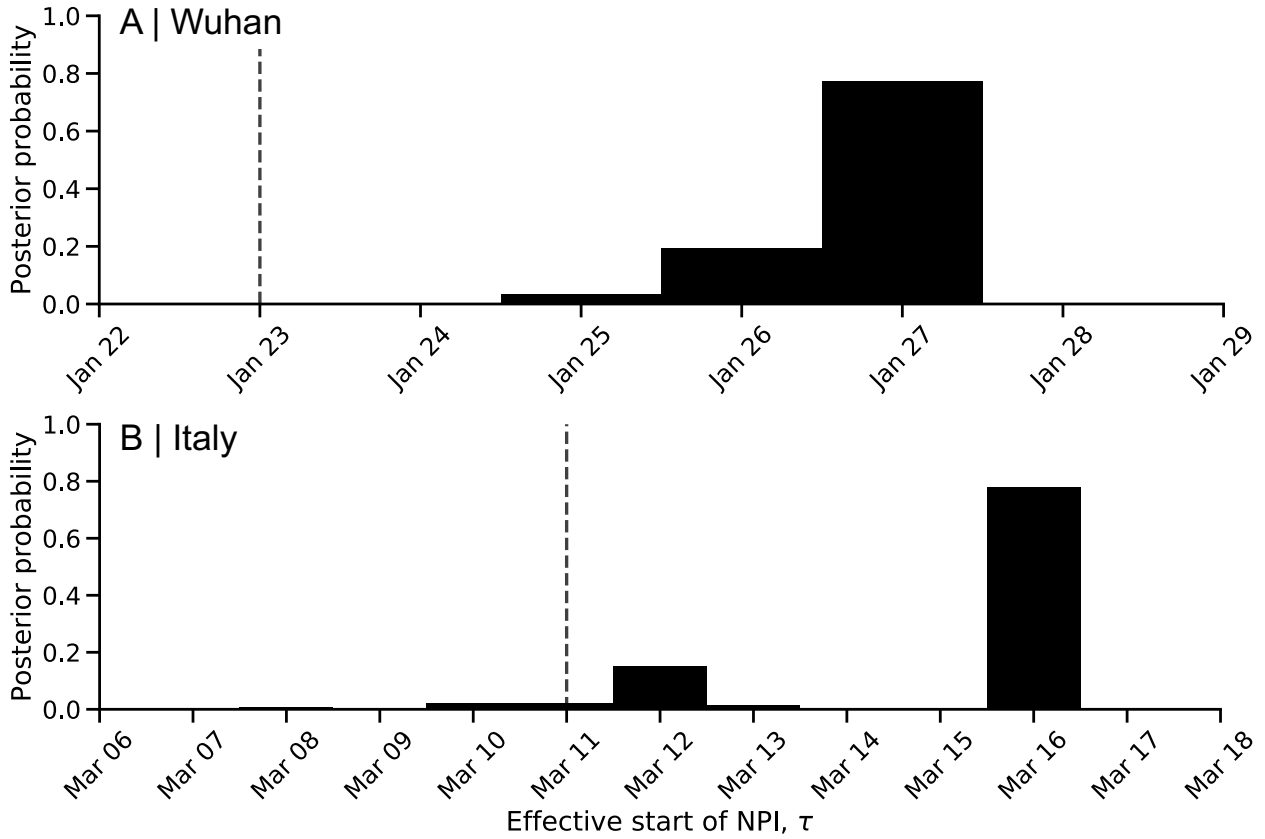


Figure 2: Delayed effect of non-pharmaceutical interventions in Italy and Wuhan, China.

127 In Italy, the first case officially confirmed on Feb 21, a lockdown was declared in Northern Italy on
 128 Mar 8, with social distancing implemented in the rest of the country, and the lockdown was extended
 129 to the entire nation on Mar 11⁷. That is, the official date τ^* is either Mar 8 or 11. However, we estimate
 130 the effective date $\hat{\tau}$ at Mar 16 (the posterior probability that τ is later than Mar 11 is $(P(\tau > \tau^*) = ???)$
 131 (Figure 2). Similarly, in Wuhan, China, lockdown was declared on Jan 23⁹, but we estimate the
 132 effective start of NPIs to be 3-4 days later $(P(\tau > \tau^*) = ???)$ (Figure 2).

133 **Advanced effective start of NPIs.** In contrast, in some regions we estimate an effective start of
 134 NPIs $\hat{\tau}$ that is *earlier* than the official date τ^* (Figure 1). For example, in Spain social distancing
 135 was encouraged starting on Mar 8⁵, but mass gatherings still occurred on Mar 8, including a march
 136 of 120,000 people for the [International Women's Day](#), and a football match between [Real Betis and](#)
 137 [Real Madrid](#) (2:1) with a crowd of 50,965 in Seville. A national lockdown was only announced on
 138 Mar 14⁵. Nevertheless, we estimate the effective start of NPI $\hat{\tau}$ at Mar 8 or 9, rather than Mar 14
 139 $(P(\tau < \tau^*) = ???)$ (Figure 3).

140 **The exception that proves the rule.** We find one case in which the official and effective dates
 141 match: Switzerland ordered a national lockdown on Mar 20, after banning public events and closing
 142 schools on Mar 13 and 14⁵. Indeed, our MAP estimate $\hat{\tau}$ is Mar 20, and the posterior distribution
 143 shows two density peaks: a smaller one between Mar 10 and Mar 14, and a taller one between Mar 17
 144 and Mar 22. It's also worth mentioning that Switzerland was the first to mandate self isolation of
 145 confirmed cases⁵.

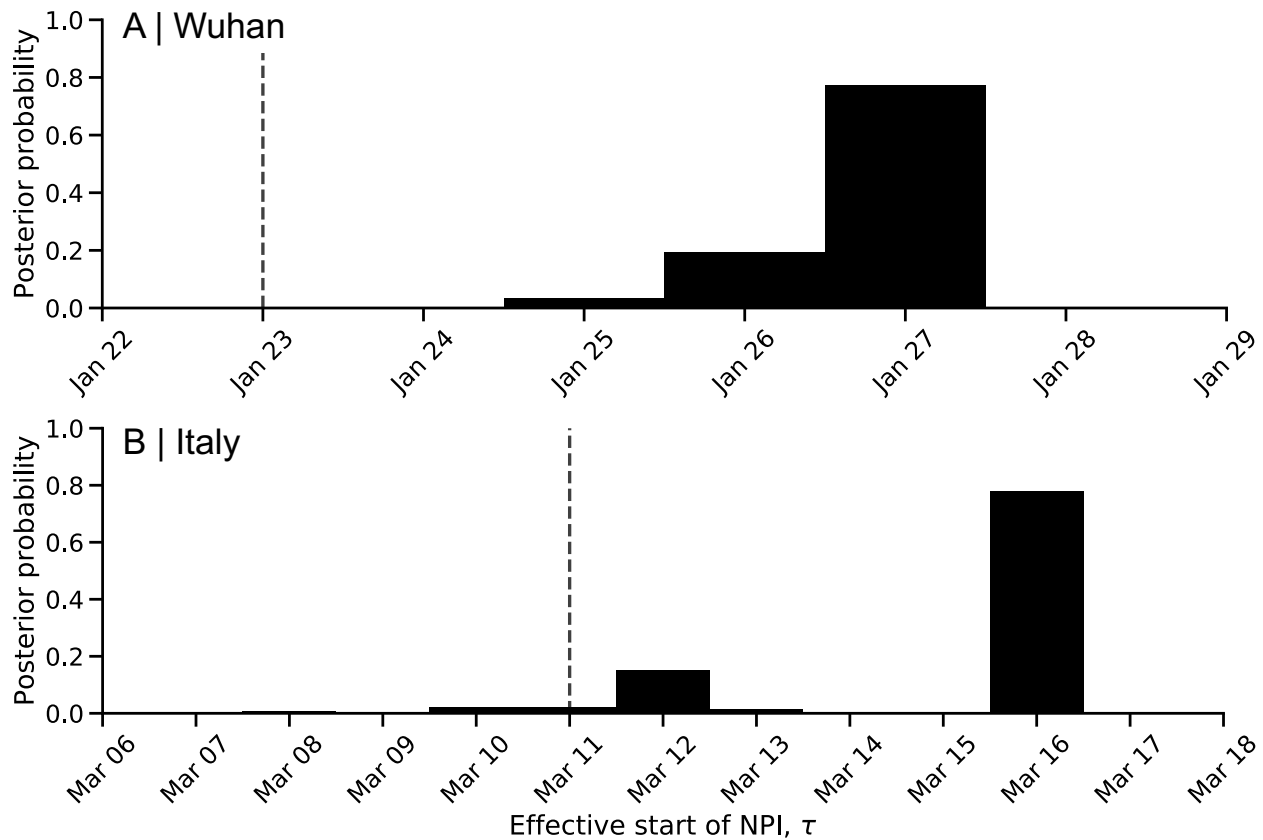


Figure 3: Advanced effect of non-pharmaceutical interventions in Spain and France.

146 **Effect of delays and advances of real-time assessment.** The success of non-pharmaceutical inter-
 147 ventions is assessed by health officials using various metrics, such as the decline in the growth rate
 148 of daily cases. These assessments are made a specific number of days after the intervention began,
 149 to accommodate for the expected serial interval (i.e. time between successive cases in a chain of
 150 transmission), which is estimated at about 4-7 days⁷. However, we hypothesize that a significant
 151 difference between the beginning of the intervention and the effective change in transmission rates
 152 invalidates assessments that assume 4-7 days. **What are good metrics for assessment of intervention**
 153 **success? growth rate of daily cases, hospitalisations, deaths?**

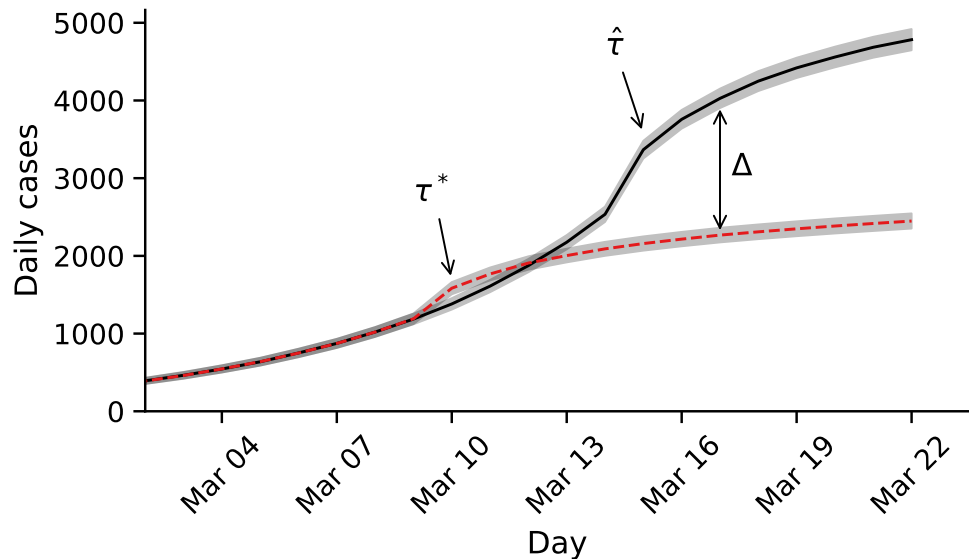


Figure 4: Delayed effective start of NPI causes leads to under-estimation of daily confirmed cases. The red and black lines show model predictions when NPIs start on the official date τ^* or on the effective date $\hat{\tau}$, respectively, with 95% confidence intervals. This demonstrates Δ the assessment error seven days after the official start of NPIs, which in this case is about 40%. Parameters are MAP estimates for Italy (TABLE).

Discussion

We have estimated the effective start date of NPIs in several geographical regions using an SEIR epidemiological model and an MCMC parameter estimation framework. We find examples of both advanced and delayed response to NPIs (Figure 1).

For example, in Italy and Wuhan, China, the effective start of the lockdowns seems to have occurred 3-5 after the official date (Figure 2). This could be explained by low compliance. In Italy, for example, a leak about the intent to lockdown Northern provinces results in people leaving those provinces⁷. However, delayed effect of NPIs could also be due to the time required by both the government and the citizens to organize for a lockdown.

In contrast, in most investigated countries, such as Spain and France, transmission rates seem to have been reduced even before official lockdowns were implemented (Figure 3). This advanced response is possibly due to adoption of social distancing and similar behavioral adaptations in parts of the population, maybe in response increased risk perception due to domestic or international COVID-19-related reports. This finding may also suggest that severe NPIs, such as lockdowns, were unnecessary, and that milder measures that were adopted by the population, possibly due to government recommendations, media coverage, and social networks, could have been sufficient for epidemic control. **check if this is true** Indeed, the evidence supports a change in transmission dynamics (i.e. a model with τ) even for Sweden, in which a lockdown was not implemented⁵, suggesting that lockdowns may not be necessary if other NPIs are adopted early enough during the outbreak (Sweden banned public events on Mar 12, encouraged social distancing on Mar 16, and closed schools on Mar 18⁵.)

As several countries (e.g. Austria, Israel) begin to relieve lockdowns and ease restrictions, we expect similar delays and advances to occur: in some countries people will begin to behave as if restrictions were eased even before the official date, and in some countries people will continue to self-restrict even after restrictions are officially removed. Such delays and advances could confuse analyses and

179 lead to wrong conclusions about the effects of NPI removals.

180 We have found that the evidence supports a model in which the parameters change at a specific
181 time point τ over a model without such a change-point. It may be interesting to investigate if the
182 evidence favors a model with *two* change-points, rather than one. Two such change-points could reflect
183 escalating NPIs (e.g. school closures followed by lockdowns), a mix of NPIs and changes in weather,
184 a mix of domestic and international effects on risk perception, or other similar factors.

185 **Conclusions.** We have estimated the effective start date of NPIs and found that they often differ
186 from the official dates. Our results emphasize the complex interaction between personal, regional,
187 and global determinants of behavioral. Thus, our results highlight the need to further study variability
188 in compliance and behavior over both time and space. This can be accomplished both by surveying
189 differences in compliance within and between populations², and by incorporating specific behavioral
190 models into epidemiological models^{1,4}.

191 **Acknowledgements**

192 This work was supported in part by the Israel Science Foundation 552/19 and 1399/17.

- [1] Arthur, R. F., Jones, J. H., Bonds, M. H. and Feldman, M. W. 2020, 'Complex dynamics induced by delayed adaptive behavior during outbreaks', *bioRxiv* pp. 1–23.
- [2] Atchison, C. J., Bowman, L., Vrinten, C., Redd, R., Pristera, P., Eaton, J. W. and Ward, H. 2020, 'Perceptions and behavioural responses of the general public during the COVID-19 pandemic: A cross-sectional survey of UK Adults', *medRxiv* p. 2020.04.01.20050039.
- [3] Dunn, A. G., Leask, J., Zhou, X., Mandl, K. D. and Coiera, E. 2015, 'Associations between exposure to and expression of negative opinions about human papillomavirus vaccines on social media: An observational study', *J. Med. Internet Res.* **17**(6), e144.
- [4] Fenichela, E. P., Castillo-Chavez, C., Ceddiac, M. G., Chowell, G., Gonzalez Parrae, P. A., Hickling, G. J., Holloway, G., Horan, R., Morin, B., Perrings, C., Springborn, M., Velazquez, L. and Villalobos, C. 2011, 'Adaptive human behavior in epidemiological models', *Proc. Natl. Acad. Sci. U. S. A.* **108**(15), 6306–6311.
- [5] Flaxman, S., Mishra, S., Gandy, A., Unwin, J. T., Coupland, H., Mellan, T. A., Zhu, H., Berah, T., Eaton, J. W., Guzman, P. N. P., Schmit, N., Cilloni, L., Ainslie, K. E. C., Baguelin, M., Blake, I., Boonyasiri, A., Boyd, O., Cattarino, L., Ciavarella, C., Cooper, L., Cucunubá, Z., Cuomo-Dannenburg, G., Dighe, A., Djaafara, B., Dorigatti, I., Van Elsland, S., Fitzjohn, R., Fu, H., Gaythorpe, K., Geidelberg, L., Grassly, N., Green, W., Hallett, T., Hamlet, A., Hinsley, W., Jeffrey, B., Jorgensen, D., Knock, E., Laydon, D., Nedjati-Gilani, G., Nouvellet, P., Parag, K., Siveroni, I., Thompson, H., Verity, R., Volz, E., Gt Walker, P., Walters, C., Wang, H., Wang, Y., Watson, O., Xi, X., Winskill, P., Whittaker, C., Ghani, A., Donnelly, C. A., Riley, S., Okell, L. C., Vollmer, M. A. C., Ferguson, N. M. and Bhatt, S. 2020, 'Estimating the number of infections and the impact of non-pharmaceutical interventions on COVID-19 in 11 European countries', *Imp. Coll. London* (March), 1–35.
- [6] Foreman-Mackey, D., Hogg, D. W., Lang, D. and Goodman, J. 2013, 'emcee : The MCMC Hammer', *Publ. Astron. Soc. Pacific* **125**(925), 306–312.
- [7] Gatto, M., Bertuzzo, E., Mari, L., Miccoli, S., Carraro, L., Casagrandi, R. and Rinaldo, A. 2020, 'Spread and dynamics of the COVID-19 epidemic in Italy: Effects of emergency containment measures', *Proc. Natl. Acad. Sci.* p. 202004978.
- [8] Kaufman, M. R., Cornish, F., Zimmerman, R. S. and Johnson, B. T. 2014, 'Health behavior change models for HIV prevention and AIDS care: Practical recommendations for a multi-level approach', *J. Acquir. Immune Defic. Syndr.* **66**(SUPPL.3), 250–258.
- [9] Li, R., Pei, S., Chen, B., Song, Y., Zhang, T., Yang, W. and Shaman, J. 2020, 'Substantial undocumented infection facilitates the rapid dissemination of novel coronavirus (SARS-CoV2)', *Science* (80-.). p. eabb3221.
- [10] Pei, S. and Shaman, J. 2020, 'Initial Simulation of SARS-CoV2 Spread and Intervention Effects in the Continental US', *medRxiv* p. 2020.03.21.20040303.
- [11] Spiegelhalter, D. J., Best, N. G., Carlin, B. P. and Van Der Linde, A. 2002, 'Bayesian measures of model complexity and fit', *J. R. Stat. Soc. Ser. B Stat. Methodol.* **64**(4), 583–616.
- [12] Wiyeh, A. B., Cooper, S., Nnaji, C. A. and Wiysonge, C. S. 2018, 'Vaccine hesitancy – Outbreaks': using epidemiological modeling of the spread of ideas to understand the effects of vaccine related events on vaccine hesitancy', *Expert Rev. Vaccines* **17**(12), 1063–1070.
- [13] Zipfel, C. M. and Bansal, S. 2020, 'Assessing the interactions between COVID-19 and influenza in the United States', *medRxiv* (February), 1–13.